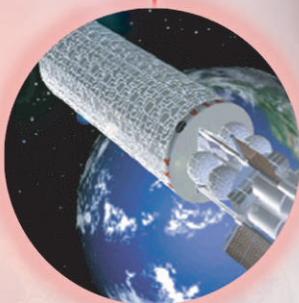


# FUSION RESEARCH AT GENERAL ATOMICS

## **ANNUAL REPORT**

**ADVANCED FUSION  
TECHNOLOGY RESEARCH  
AND DEVELOPMENT**



**OCTOBER 1, 2000  
THROUGH  
SEPTEMBER 30, 2001**

 **GENERAL ATOMICS**

GA-A23869

**ADVANCED FUSION TECHNOLOGY  
RESEARCH AND DEVELOPMENT**

**ANNUAL REPORT TO THE  
U.S. DEPARTMENT OF ENERGY**

**OCTOBER 1, 2000 THROUGH SEPTEMBER 30, 2001**

**by  
PROJECT STAFF**

**Work supported by  
U.S. Department of Energy  
under Contract No. DE-AC03-98ER54411**

**GENERAL ATOMICS PROJECT 30007  
DATE PUBLISHED: OCTOBER, 2002**

## DISCLAIMER

This report was prepared as an account of work sponsored by an agency of the United States Government. Neither the United States Government nor any agency thereof, nor any of their employees, makes any warranty, express or implied, or assumes any legal liability or responsibility for the accuracy, completeness, or usefulness of any information, apparatus, product, or process disclosed, or represents that its use would not infringe privately owned rights. Reference herein to any specific commercial product, process, or service by trade name, trademark, manufacturer, or otherwise, does not necessarily constitute or imply its endorsement, recommendation, or favoring by the United States Government or any agency thereof. The views and opinions of authors expressed herein do not necessarily state or reflect those of the United States Government or any agency thereof.

This report has been reproduced  
directly from the best available copy

Available to DOE and DOE contractors from the  
Office of Scientific and Technical Information  
P.O. Box 62  
Oak Ridge, TN 37831  
Prices available from (615) 576-8401,  
FTS 626-8401

Available to the public from the  
National Technical Information Service  
U.S. Department of Commerce  
5285 Port Royal Road  
Springfield, VA 22161

Cover Photo: Cover of spin-off brochure "The Surprising Benefits of Creating a Star" (see Section 10).  
Top inset: NASA illustration of magnetized target fusion propulsion. Middle inset: University of Rochester Laboratory for Laser Energetics image of a target implosion in the OMEGA target chamber. Bottom inset: Los Alamos National Laboratory photo showing diamond-like carbon coatings being applied to automotive pistons.

# CONTENTS

1.	ADVANCED FUSION TECHNOLOGY RESEARCH AND DEVELOPMENT OVERVIEW .....	1-1
2.	FUSION POWER PLANT DESIGN STUDIES (ARIES).....	2-1
	Background.....	2-1
	Target Thermal Survivability .....	2-1
	Target Filling and Metallic Films .....	2-1
	Fluidized Bed.....	2-2
	Target Drag and In-Chamber Tracking .....	2-3
	Conferences/Meetings .....	2-3
3.	IFE TARGET SUPPLY SYSTEM DEVELOPMENT .....	3-1
	Background.....	3-1
	FY01 Scope and Objectives.....	3-1
	Target Injection and Tracking System Preliminary Design .....	3-2
	Metallic Foams .....	3-2
	Thin Film Deposition and Optical Property Measurements .....	3-2
	References.....	3-4
	Conferences/Meetings .....	3-6
	Publications/Reports .....	3-7
4.	NEXT STEP FUSION DESIGN .....	4-1
	Physics .....	4-1
	Engineering.....	4-3
	Thermal Analysis of FIRE Outer Divertor .....	4-5
	Parameters.....	4-5
	Geometry .....	4-6
	Results.....	4-6
5.	ADVANCED LIQUID PLASMA-FACING SURFACES (ALPS) .....	5-1
	Tokamak Experiments .....	5-1
	Li-DiMES Modeling.....	5-2
	Atomic Data Coordination.....	5-3
	Conferences/Meetings .....	5-3
	Publications/Reports .....	5-3

## CONTENTS (Continued)

6.	ADVANCED POWER EXTRACTION STUDY (APEX) .....	6-1
	Evolve Design .....	6-1
	SiC <sub>f</sub> /SiC-LiPb Design Assessment .....	6-2
	Chamber Technology Peer Review .....	6-3
	Planning for FY02 .....	6-3
	Conferences/Meetings .....	6-3
7.	PLASMA INTERACTIVE MATERIALS (DiMES) .....	7-1
	Li Experiment .....	7-1
	Experimental Background .....	7-1
	Experimental Data .....	7-2
	Summary .....	7-6
	Scrape-Off Layer Measurement .....	7-7
	Solid Target Experiments .....	7-7
	Disruption Mitigation .....	7-7
	W-Rod Experiment .....	7-8
	Planning for FY02 .....	7-8
	Conferences/Meetings .....	7-8
	Publications/Reports .....	7-8
8.	VANADIUM COMPONENT DEMO .....	8-1
	Conferences/Meetings .....	8-1
	Publications/Reports .....	8-1
9.	RF TECHNOLOGY .....	9-1
	Compline Antenna .....	9-1
	Advanced ECH Launcher Development .....	9-1
	Window Validation .....	9-4
	International Collaboration .....	9-5
	Conferences/Meetings .....	9-6
10.	SPIN-OFF BROCHURE .....	10-1

## LIST OF FIGURES

3.1.	Fast gas propellant valve mechanical design .....	3-2
3.2.	Low density foams have been recently fabricated at LANL .....	3-3
3.3.	Gold reflectivity sample geometry .....	3-3
3.4.	Normal reflectivity versus wavelength for gold layered on GDP .....	3-4
3.5.	Calculated reflectivity of a gold layer on silicon averaged over all angles as a function chamber wall temperature for various gold layer thicknesses .....	3-5
3.6.	Outer ablator temperature rise versus chamber temperature for various gold layer thicknesses .....	3-5
4.2.1.	Features of FIRE Baseline .....	4-4
6-1.	Schematics of the poloidal flow transpiration cooled EVOLVE FW/blanket design .....	6-2
7-1.	Upper frame: tile current array monitor signals in the row 13 tiles during the termination phase of shot 105511. Lower Frame: plasma current during the final 85 ms of the shot .....	7-3
7-2.	Upper frame: locked mode detector signals pr12 and pr13 show the onset of a growing locked mode at 3452 ms. Lower frame: $D_{\alpha}$ recycling light from filterscope chord looking near the DiMES probe shows an increase in recycling as the locked mode grows after 3455 ms .....	7-5
9-1.	Photograph of the prototype graded CCD/CFC mirror and flexible carbon fiber bundle under development for use in advanced long pulse ECH launcher mirrors .....	9-2
9-2.	Experimental set-up at JAERI for high power testing of the 170 GHz remotely-steerable launcher apparatus .....	9-3
10-1.	Cover of spin-off brochure .....	10-1

## LIST OF TABLES

4.3.1.	Physical parameters .....	4-5
4.3.2.	Power flows .....	4-6
4.3.3.	Analysis results for two geometries .....	4-7

Section 1

---

**ADVANCED FUSION TECHNOLOGY RESEARCH AND  
DEVELOPMENT OVERVIEW**

# 1. ADVANCED FUSION TECHNOLOGY RESEARCH AND DEVELOPMENT OVERVIEW

The General Atomics (GA) Advanced Fusion Technology program seeks to advance the knowledge base needed for next-generation fusion experiments, and ultimately for an economical and environmentally attractive fusion energy source. To achieve this objective, we carry out fusion systems design studies to evaluate the technologies needed for next-step experiments and power plants, and we conduct research to develop basic and applied knowledge about these technologies. GA's Advanced Fusion Technology program derives from, and draws on, the physics and engineering expertise built up by many years of experience in designing, building, and operating plasma physics experiments. Our technology development activities take full advantage of the GA DIII-D program, the DIII-D facility and the Inertial Confinement Fusion (ICF) program and the ICF Target Fabrication facility.

The following sections summarize GA's FY01 work in the areas of Fusion Power Plant Studies (ARIES, Section 2), Inertial Fusion Energy Target Supply System Development (Section 3), Next Step Fusion Design (Section 4), Advanced Liquid Plasma Facing Surfaces (ALPS, Section 5), Advanced Power Extraction Study (APEX, Section 6), Plasma Interactive Materials (DiMES, Section 7), Vanadium Component Demonstration (Section 8), RF Technology (Section 9) and Spin-offs Brochure (Section 10). Our work in these areas continues to address many of the issues that must be resolved for the successful construction and operation of next-generation experiments and, ultimately, the development of safe, reliable, economic fusion power plants.

Our work was supported by the Office of Fusion Energy Sciences, Facilities and Enabling Technologies Division, of the U.S. Department of Energy.

**Section 2**

---

**FUSION POWER PLANT DESIGN STUDIES (ARIES)**

## 2. FUSION POWER PLANT DESIGN STUDIES (ARIES)

### BACKGROUND

The ARIES Program is a multi-institutional activity to explore and develop the commercial potential of fusion as a future energy source. This is accomplished through integrated systems studies of both MFE and IFE power plant concepts. General Atomics' task is to provide target injection and target fabrication input to the ARIES-IFE integrated system studies.

We participated in the ARIES IFE meetings listed in the following sections as well as monthly conference calls. We provided updates on target fabrication and injection research and participated in target and chamber design guidelines as they affect target fabrication and injection. In this regard we often reported work that is ongoing regardless of funding source.

### TARGET THERMAL SURVIVABILITY

Materials measurement equipment is being designed to verify ability to withstand required acceleration. Analysis has been performed to assess the capability of the direct drive and indirect drive targets to survive the thermal chamber environment. Results for the indirect drive target show minimal DT heating during injection and transit. It was determined that the initial Sombrero (chamber gas and wall) conditions resulted in excessive direct drive target heating. Removal of the attenuating chamber gas widens the design window and may allow target injection without excessive target heating. A sabot is used to protect the direct drive target target during acceleration and is removed prior to entering the chamber. Other, more speculative, approaches such as a wake shield, outer frost coating, and a sabot that is removed in the last few milliseconds were also considered.

### TARGET FILLING AND METALLIC FILMS

Permeation appears workable for large scale filling for both polymer capsule indirect drive targets and direct drive targets (but optimization or a faster method would be helpful). Liquid injection filling through micro-needles was evaluated. It was determined that needle sizes of  $< 0.5 \mu\text{m}$  are required to avoid subsequent hole plugging but needles this small would provide insufficient filling rate. Hole plugging is required for larger

needle sizes, but no adequate hole plugging method has been identified. An alternate liquid flooding fill method will require hole plugging for indirect drive and possibly for direct drive. This method also needs work on ideas to control filling level.

To address the question of permeation fill times for gold-coated capsules, PAMS mandrels were sputter coated with gold in a bounce pan and gas permeation rates were measured. Shells with 250 Å gold layers took about 10 times longer to fill than uncoated shells, indicating that the gold-coating process needs optimization to decrease the fill time.

A Pd-coated target is easier to fill than a gold-coated target because of the higher Pd hydrogen permeability. We coated flat surfaces and shells with 300 Å to 1200 Å of palladium. We measured the optical properties ( $n$  and  $k$ ) of the palladium on the flat surfaces as a function of wavelength. We related this data to dry-wall chamber operating conditions by modeling the reflectivity as a function of blackbody radiation spectrum. The normal incidence wavelength integrated reflectivity of a 300 Å layer on GDP was 76% for a chamber wall temperature of 1480°C, 79% at 1000°C, and 82% at 627°C.

## **FLUIDIZED BED**

Fluidized bed coating of GDP shells has shown reproducible thickness and coating rates with shell to shell thickness variations of about 10% – roughly the same as for ICF (small batch) coating methods. Solution spray drying in a fluidized bed is also being tested as a target coating method. We were able to produce free-standing polyimide coatings in a fluidized bed with just a few weeks of effort. The first coatings are rough and vapor smoothing is being investigated. We are evaluating cryogenic fluidized bed layering of targets with LANL and Schafer personnel. Fluidized bed design calculations show that it is difficult to provide the very small  $\Delta T$  (from the bottom to the top of the bed) that is normally associated with layering. However, larger temperature variations may be acceptable in a fluidized bed since the targets are moving rapidly and randomly and the target's transition through many temperature regions in a short time period. Other options, such as internal cooling tubes within the fluidized bed may also be used to equalize the temperature. We are also evaluating the addition of HD or H<sub>2</sub> mist or D<sub>2</sub> “snowballs” to the bed to equalize temperature, and the use of a rotary kiln for continuous delivery of targets. Room temperature layering experiments with oxalic acid as substitute for hydrogen are also being conducted to gain actual operational experience with a fluidized bed for layering. These surrogate experiments are also intended to give us sufficient confidence to proceed with the design and construction of cryogenic fluidized bed system for layering.

## TARGET DRAG AND IN-CHAMBER TRACKING

Target drag due to chamber gas was reviewed to determine the conditions that would require in-chamber target tracking. For a 2 mm radius, 4 mg target, moving 400 m/s through a xenon background gas, the gas pressure must be known to approximately  $\pm 5 \times 10^{-6}$  Torr to avoid in-chamber tracking. Therefore, in chamber tracking will probably be required for direct drive targets traveling through chambers with the expected gas densities of 5 to 50 mTorr. Our baseline in-chamber tracking method is similar to our external position measurement method. It utilizes a collimated light source that passes through the chamber intersecting the target path at right angles and landing on a photodiode array. The target blocks a portion of the light from hitting the photodiode allowing target position detection. The feasibility of an interferometric in-chamber tracking system is being investigated by Physical Optics Corporation under a DOE-funded SBIR Grant. This relative tracking system would require precise initial position information (i.e., from the ex-chamber tracking system).

## CONFERENCES/MEETINGS

1. ARIES-IFE study meeting on December 5–6, 2000, San Diego, California.
2. ARIES-IFE study meeting on March 8–9, 2001, Livermore, California.
3. ARIES Town Meeting on Tritium and the DT Fuel Cycle on March 6–7, 2001, Livermore, California.
4. ARIES-IFE study meeting on June 7–8, 2001, San Diego, California.

**Section 3**

---

**IFE TARGET SUPPLY SYSTEM DEVELOPMENT**

## 3. IFE TARGET SUPPLY SYSTEM DEVELOPMENT

### BACKGROUND

The overall purpose of this task is to address issues associated with the target supply system for a future IFE power plant. This includes the major areas of target fabrication,<sup>1</sup> injection, and tracking. The long-term workscope for this task is to address the following issues:

- Ability to economically fabricate, fill, and layer targets that meet IFE requirements
- Ability of targets to withstand acceleration into the reaction chamber.
- Ability of targets to survive in the chamber environment (heating due to radiation and gases)
- Accuracy and repeatability of target injection
- Ability to accurately track targets

### FY01 SCOPE AND OBJECTIVES

The FY01 GA work scope for this task is focused on (a) understanding the scientific basis for target injection and (b) initiating the preliminary design of a new injection and tracking system for higher precision, multi-shot, injections of direct and indirect drive targets. We are also continuing analysis of issues associated with target injection, tracking, and fabrication.

We hosted an indirect drive target workshop on May 1, 2001. A subcontract has been issued for Oak Ridge National Laboratory to design, build, and test the fast operating target injection propellant valve. Additional funding has been obtained from the Naval Research Laboratory (NRL) to complete the preliminary and final target injector designs and for additional target fabrication research. Most of the remaining target injector design has been performed under the new contract.

Brief highlights of the FY01 progress and accomplishments are covered in the following sections.

---

<sup>1</sup>GA is supporting Los Alamos National Laboratory (LANL), which is the lead lab for target fabrication.

## TARGET INJECTION AND TRACKING SYSTEM PRELIMINARY DESIGN

The preliminary design was successfully completed on schedule in July. The preliminary design review committee recommended relatively minor changes which have since been incorporated into the design. Much of the preliminary design work and all of the final design work were completed under the NRL contract and are reported through other channels.

Analyses to determine the valve size to meet specifications were completed. To meet the valve throughput requirements for helium gas, in both the high pressure (415 psi inlet, 21 psid pressure drop) and low pressure (83 psi inlet, 4 psid pressure drop) cases, requires an orifice diameter of about 21 mm. The power supply is being fabricated and the pressure and shock sensors for the valve have been ordered. The valve mechanical design is in progress and illustrated in Fig. 3.1.

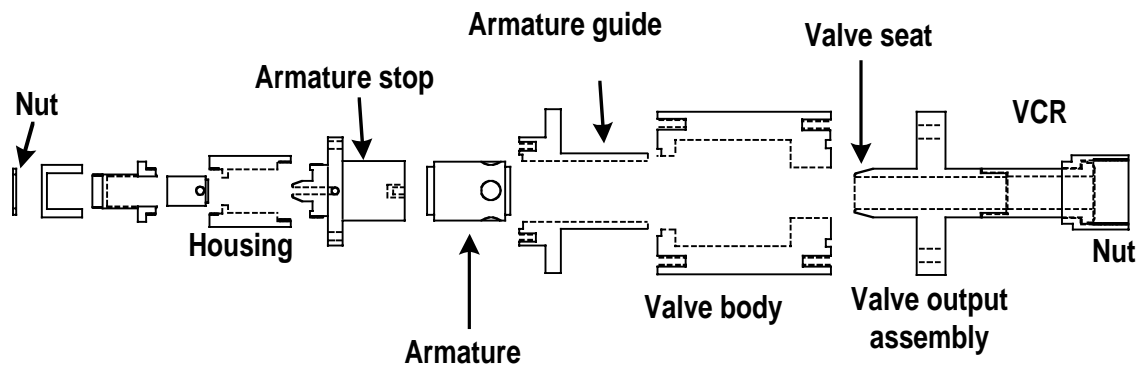


Fig. 3.1. Fast gas propellant valve mechanical design.

## METALLIC FOAMS

Much of the LLNL indirect drive HIF target design consists of low-density foams. Initial samples of low-density (30 mg/cc) gold and tungsten doped polystyrene foams have been fabricated at Los Alamos National Laboratory (Fig. 3.2).

## THIN FILM DEPOSITION AND OPTICAL PROPERTY MEASUREMENTS

The current radiation preheated direct drive target design has a very thin ( $\sim 300 \text{ \AA}$ ) outer gold layer to preheat the ablator, making the target more stable to hydrodynamic instabilities. This gold layer can also reduce target heating while transiting the reaction chamber by increasing the target thermal reflectivity. Based on calculations for bulk gold

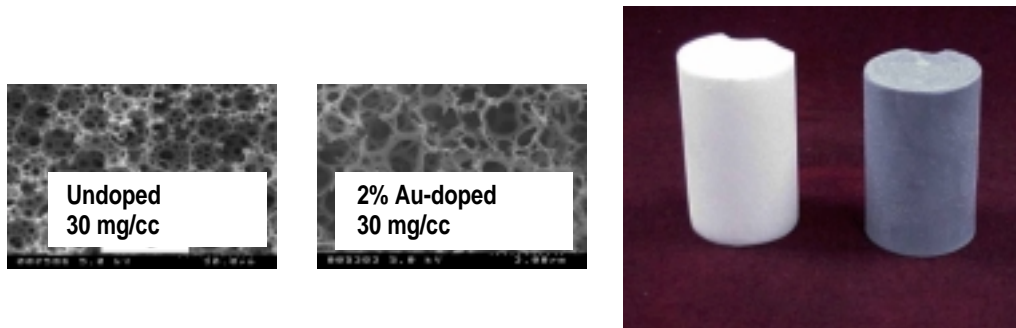


Fig. 3.2. Low density foams have been recently fabricated at LANL.

reflectivity [1], we previously assumed reflectivity value of 98% (averaged over all angles and a black-body spectrum) in our target heating calculations. However, the layer thickness, the deposition process, and even the substrate can affect the gold reflectivity. To help determine the reflectivity that we can expect from a gold coated target, we prepared three samples, each with a layer of Glow Discharge Polymer (GDP) target shell material on a silicon substrate, and varying thickness of gold ( $\sim 600$ ,  $800$ , and  $1250 \text{ \AA}$ )<sup>2</sup> as shown in Fig. 3.3.

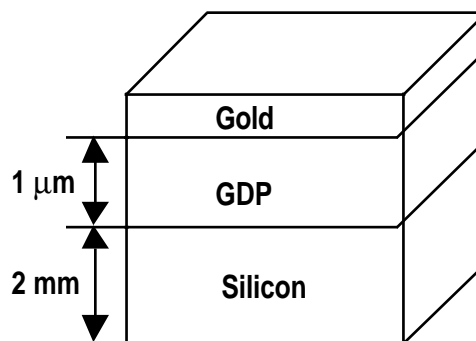


Fig. 3.3. Gold reflectivity sample geometry.

J.A. Woollam company performed spectroscopic ellipsometry measurements on the samples. Based on the ellipsometry measurements, they calculated  $n$  and  $k$  values and layer thicknesses for the gold and GDP.

Based on the calculated  $n$  and  $k$  values and layer thicknesses, we calculated the normal reflectivity of the gold layers on a GDP substrate. The calculated reflectivity for each sample thickness versus wavelength, along with the calculated reflectivity for bulk

<sup>2</sup>This range of values was selected for initial analysis because it was calculated that 98% reflectivity would require a gold thickness of approximately  $1000 \text{ \AA}$ .

gold (based on literature values for  $n$  and  $k$ ), is plotted in Fig. 3.4. These values are encouraging because they show that high reflectivity is achievable using our gold deposition process, especially for wavelengths greater than  $2\ \mu\text{m}$ .

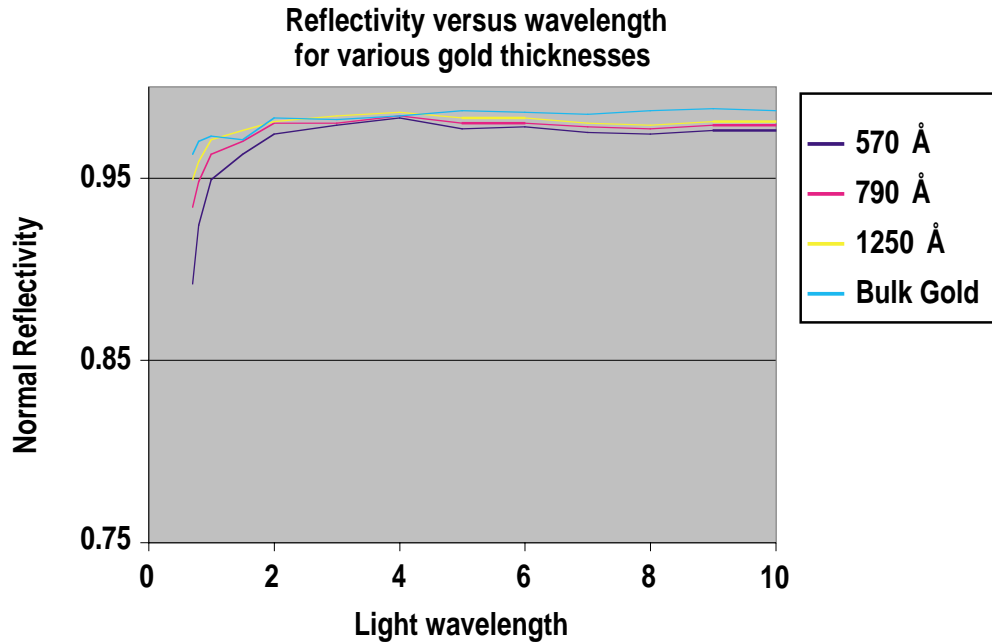


Fig. 3.4. Normal reflectivity versus wavelength for gold layered on GDP.

We extended the reflectivity analysis to multi-layer calculations over more angles of incidence and averaged the results over black body spectrums to determine the validity of the assumed 98% target reflectivity.

Based on the calculated  $n$  and  $k$  values for a  $570\ \text{\AA}$  layer, we calculated the reflectivity of a  $300\ \text{\AA}$  layer averaged over all angles and a black body spectrum as a function of temperature. UCSD extended our results for various layer thicknesses as shown in Fig. 3.5. We then calculated target heating vs gold thickness and chamber temperature as shown in Fig. 3.6.

## REFERENCES

- [1] Program Status, 1st Quarter – FY00, Advanced Fusion Technology, General Atomics Report GA-C19572, (2000).

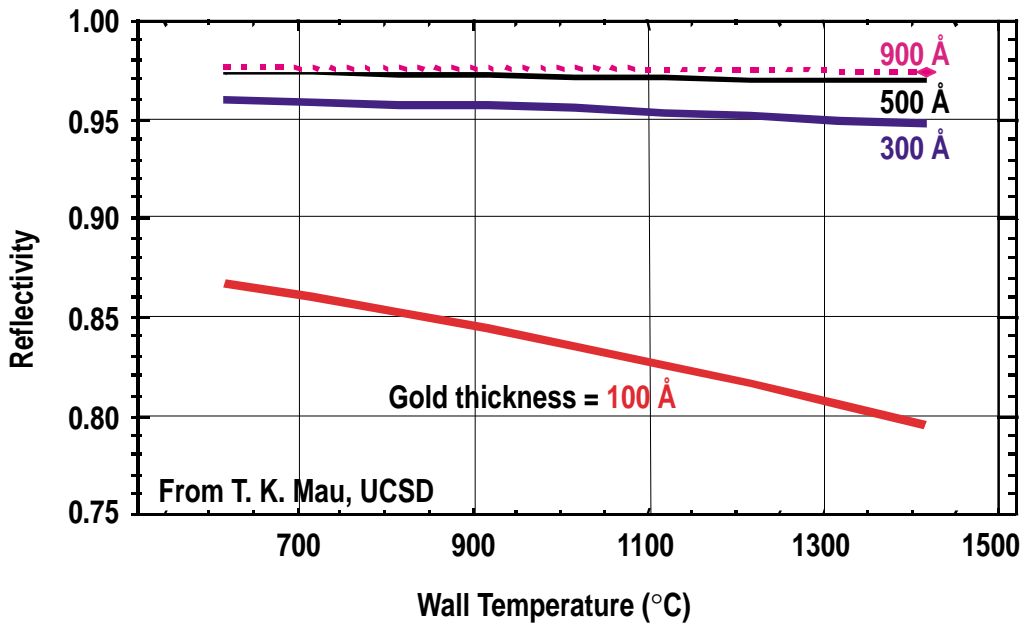


Fig. 3.5. Calculated reflectivity of a gold layer on silicon averaged over all angles as a function chamber wall temperature for various gold layer thicknesses.

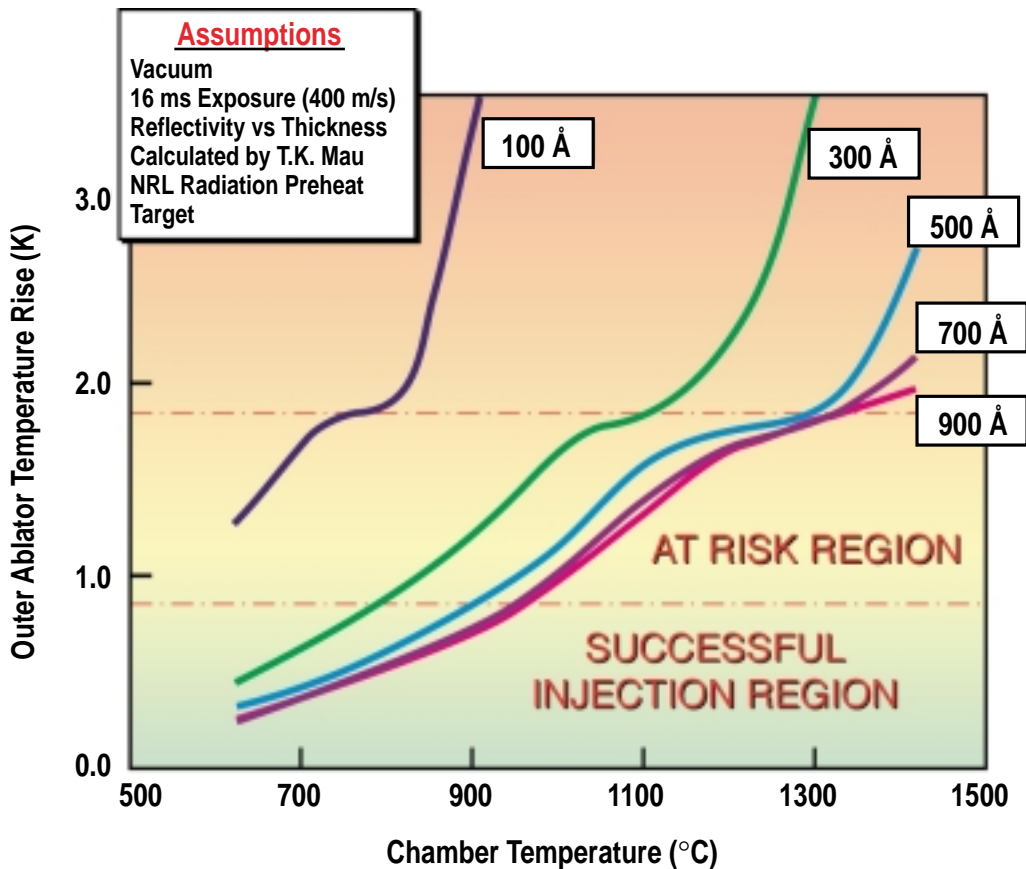


Fig. 3.6. Outer ablator temperature rise versus chamber temperature for various gold layer thicknesses.

## CONFERENCES/MEETINGS

- GA participated in the 14th Topical Meeting on the Technology of Fusion Energy, Park City, Utah, October 15–19. We presented the paper “Design of an Inertial Fusion Energy Target Tracking and Position Prediction System.”
- A joint GA-LANL workshop on Tritium in Target Fabrication Facility (TFF) was held at Los Alamos in November. We concluded that it is necessary to keep TFF tritium inventories less than ~1 kg, and desirable to keep releasable inventories less than 250 g. These values would be substantially exceeded by in-hohlraum filling of indirect drive targets and room temperature filling of direct drive targets. Potential methods to decrease tritium inventories include:
  - Increase diffusion fill temperature from room temperature to about 400°C, thereby decreasing fill time.
  - Fill indirect drive targets prior to assembly in the hohlraum (requires cryogenic assembly of the filled capsule and the hohlraum).
  - Use infrared or rf heating to reduce target-layering time.
- GA hosted an indirect drive target workshop in May with participants from LLNL, LANL, Schafer, ANL and UCSD. GA participants made presentations on “Target Injection and Tracking Interfaces,” and “Surface Finish and Material Properties of IFE Ablators.”
  - The target injection interface presentation described the requirements imposed on the target by the injection process, noting that most target material properties are currently unknown. Experimental equipment designs are being prepared to measure DT strength at LANL under conditions relevant to target injection. Indirect drive target DT heating during the injection process is calculated to be very small. A counter flowing gas and shutter method was presented to keep Flibe vapors out of the tracking system. The status of the injection and tracking system design was also presented.
  - The materials properties presentation described the properties of beryllium, polyimide, and CH (glow discharge polymer – GDP) capsules. It described the GDP capsule fabrication process and target characterization methods.

A process to select a hohlraum wall material for the heavy ion beam driven target design was developed at the workshop, involving a multi-disciplinary optimization over several organizations.

- GA participated in an IAEA-sponsored research coordination meeting for “Elements of Power Plant Design for Inertial Fusion Energy” held in Vienna in May. The purpose of the meeting was to promote inertial fusion energy development by improving international cooperation. Eighteen scientists and engineers from ten countries were in attendance. A paper and abstract were prepared and delivered for the meeting documentation, and a presentation covering IFE target fabrication, injection, and tracking activities in the U.S. was given. It was agreed the next meeting would be at GA in July of 2002.
- GA participated in the Heavy Ion Fusion Meeting at LLNL in July. We gave presentations entitled “Indirect Drive Target Injection,” “Summary of Target Design, Target Fabrication, and Chamber Workshop,” “Heavy Ion Fusion and General Atomics,” and contributed to the presentation “Progress on IFE Target Fabrication” made by LANL staff.

Target steering, possibly using ion beam charging of targets, was discussed. Target structure and target heating for gas gun injection were presented. Analysis indicates that 2 g indirect-drive targets could be accurately delivered ( $\pm 0.3$  mm axial) within a 3 m radius chamber containing xenon gas known to an accuracy of  $\pm 0.2$  Torr without in-chamber tracking.

## PUBLICATIONS/REPORTS

1. R.W. Petzoldt, M. Cherry, N.B. Alexander, D.T. Goodin, G.E. Besenbruch, and K.R. Schultz, “Design of an Inertial Fusion Energy Target Tracking and Position Prediction System,” *Fusion Technology*, Vol. **39**, (2001), 678.
2. A. Nobile, P. Gobby, A.M. Schwendt, W.P. Steckle, J.K. Hoffer, D.T. Goodin, G.B. Besenbruch, and K.R. Schultz, “Concepts for Fabrication of Inertial Fusion Energy Targets,” *Fusion Technology*, Vol. **39**, (2001), 684.
3. J.F. Latkowski, S. Reyes, G.E. Besenbruch, and D.T. Goodin, “Preliminary Safety Assessment for an IFE Target Fabrication Facility,” *Fusion Technology*, Vol. **39**, (2001), 960.

4. D.T. Goodin, N.B. Alexander, C.R. Gibson, A. Nobile, R.W. Petzoldt, N.P. Siegel, L. Thompson, “Developing Target Injection and Tracking for Inertial Fusion Energy Power Plants,” *Nucl. Fusion*, **41**, No. 5, (2001) 527.
5. D.T. Goodin, C.R. Gibson, R.W. Petzoldt, N.P. Siegel, L. Thompson, A. Nobile, G.E. Besenbruch, and K.R. Schultz, “Developing the Basis for Target Injection and Tracking in Inertial Fusion Energy Power Plants,” Accepted for publication in *Fusion Engineering and Design*.
6. K.R. Schultz, D.T. Goodin, A. Nobile, “IFE Target Fabrication and Injection – Achieving Believability,” *Nuclear Instruments and Methods in Physics Research*, Section A, 464, (2001) 109.

## Section 4

---

# NEXT STEP FUSION DESIGN

## 4. NEXT STEP FUSION DESIGN

This task provides physics analysis, engineering analysis and other scientific and technical input to Next Step Options (NSOs) Studies for the U.S. Fusion Science Program. Emphasis in this work is on options (design candidates) to obtain plasma behavior at high energy gain and for long duration operation pulses. The FY01 effort was comprised of three tasks, described in the following sections: Physics; Engineering; and Thermal Analysis of the FIRE Outer Divertor.

### 4.1. PHYSICS

The principal content of the Physics Task is to provide definition of physics and plasma operation objectives, physics and plasma science assessments and definition of physics and other design requirements for U.S. NSO studies. Activity for this task comprises an approximately 0.1 FTE effort and has been conducted on an approximately constant level-of-effort basis. John Wesley is the principal and sole investigator at General Atomics.

Activities during FY01 included participation in weekly FIRE (Fusion Ignition Research Experiment) engineering conference calls and representation of general U.S. burning plasma science interests in the two University Fusion Association (UFA) Burning Plasma Science Workshops held in Austin in December 2000 and in San Diego in May 2001. The first Workshop focused on definition and discussion of generic “burning plasma science” issues; the second Workshop focused on generic technology issues for candidate burning plasma science experiments (BPSXs) and presentation of specific BPSX candidate concepts (FIRE, Ignitor and ITER-FEAT). Technical contributions were made to the first Workshop on the subjects of “disruption physics.” Wesley acted as the on-site organizer for the second workshop. Summaries and presentations from the workshop are now archived at <http://fusion.gat.com/bps2/>.

Activities in the 4th quarter of FY01 shifted to participation in the Preliminary Organizing Committee meeting for the 2002 Fusion Science Summer Study (aka Snowmass 2002) to be held at Snowmass Village, Colorado, in July 2002. Preparations are being made for Wesley to co-chair the MFE “Physics Operations” Working Group. The Snowmass 2002 website on the Fusion “lithos” server is being set up with support from Fusion Group computer personnel.

## 4.2. ENGINEERING

The Fusion Ignition Research Experiment (FIRE) is being studied as a possible Next Step Option in the U.S. fusion program. The purpose of this task is to provide engineering management and technical input. This is a continuing effort performed by R.J. Thome of GA as Engineering Manager for NSO FIRE. Physics Management for FIRE is done by D. Meade (PPPL), and overall Management by J. Schmidt (PPPL). Engineering Reports were issued in FY99, FY00 and the FY01 report is about to be issued. This material, as well as other related items, is available on the PPPL web site at <http://fire.pppl.gov>.

The FIRE pre-conceptual design is considering pulsed, liquid nitrogen cooled, copper toroidal and poloidal field coils. Configurations with: 1) wedged TF coils and a free standing Central Solenoid and 2) TF coils that are wedged and also bucked against the outer diameter of the Central Solenoid, are under consideration. The wedged option allows fields of 10 T to be achieved for pulse lengths of 20 s, but requires the inboard legs of the TF coils to use BeCu; the bucked and wedged option allows the use of OFHC copper throughout the TF coils which, in turn, allows the pulse lengths to increase to 31 s with a substantially lower power requirement.

Cost estimates for the wedged baseline case have been generated with input from industry and variations around the baseline have been considered using a systems code. An engineering review was held in June, 2001 at PPPL, in which independent reviewers provided comments on the following areas: TF coils, PF coils, Structures, Vacuum Vessel, Divertor, Plasma Facing Components, and Fueling and Pumping. A copy of the reviewers report to Charles Baker, VLT Director, is available on the FIRE web site. The reviewers had very favorable comments on the depth of analyses performed at this stage of design and also provided written comments on specific areas that will be determined by the project for disposition in the near to moderate term, consistent with availability of resources. The review committee recommended an increase in team resources to continue design development and to expeditiously engage in the R&D necessary to support the design effort.

A presentation of the physics and engineering aspects of FIRE was given to the Next Step Options Program Advisory Committee in Madison, Wisconsin in July, 2001. The PAC-3 endorsed the design point goals for FIRE as embodied in the 7.7 MA, 10 T baseline design. The wedged TF coil design has been tentatively selected because it satisfies the mission requirements, is more straightforward to assemble, and has more

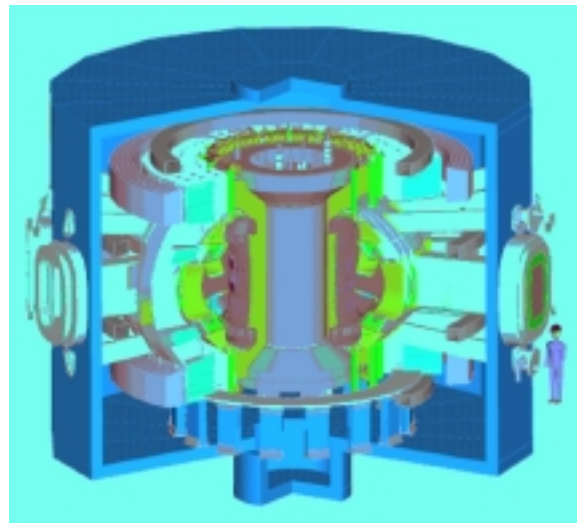
favorable remote handling features for the central solenoid. Several recommendations were made by PAC, including a recommendation that “It is important to maintain a strong, focused effort on the FIRE physics and engineering studies.”

Results of the FIRE studies indicate that a compact burning plasma experiment can be developed for a cost of about \$1.2B and that it is an attractive candidate for the next step in a fusion sciences program.

Figure 4.2.1 shows key features of the FIRE baseline design.

### Fig. 4.2.1. FEATURES OF FIRE BASELINE

- 16 wedged TF coils
- Two pairs of external divertor coils
- Two pairs of external ring coils
- Free-standing, segmented central solenoid
- Vacuum vessel filled with steel/water for shielding
- Plasma facing components:
  - Be coated Cu first wall
  - W pin-type inner divertor, baffle and out divertor
- Two outboard poloidal limiters
- Internal passive and active stabilization coils
- Remote maintenance
- 16 large midplane ports
- 32 angled ports



- 32 vertical ports
- Thermal shield
  - SS frame with SS skin
  - Insulated exterior
  - Provides 80–90 K inside

### 4.3. THERMAL ANALYSIS OF FIRE OUTER DIVERTOR

Thermal stress analysis of FIRE divertor shows that the thermal stresses in copper and assembly pins are too high in the reference design. These stresses can be reduced the by a combination of the following measures:

1. Reducing the distance between coolant channels and PFC.
2. Connecting all channels in series.
3. Moving the flow inlet to high heat flux end of the divertor.
4. Increasing the flow rate.
5. Increasing the diameter of the assembly pins.
6. Making the assembly more flexible.

The first in the list, reducing the distance between the coolant channels and PFC, was analyzed as described below. A parametric study combining all of the measures will be done in FY02.

#### 4.3.1. PARAMETERS

The physical parameters are shown in Table 4.3.1 and the power flows are shown in Table 4.3.2.

**TABLE 4.3.1**  
**Physical Parameters**

Heat Sink	Cu-Cr-Zr
PFC	Tungsten Rods, 0.125" diameter at 0.128" pitch (86.5% volume fraction)
Height	5 mm
Water Inlet temperature	30°C
Inlet Pressure	1.5 MPa
Number of Modules	32

**TABLE 4.3.2  
Power Flows**

	<b>Outer Divertor</b>
Total Power (MW)	34.3
Peak Power/module (MW)	2.32
Peak Heat Flux (MW/m <sup>2</sup> )	25.0
Nuclear heating in W (W/cm <sup>3</sup> )	42
Nuclear heating in Cu (W/cm <sup>3</sup> )	16

Incident heat flux distribution was calculated by Ulrickson with a peak value of 25 MW/m<sup>2</sup>.

### **4.3.2. GEOMETRY**

There are 32 modules in the outer divertor. Each module is 0.67 m in the toroidal direction and 0.55 m in the poloidal direction. Each module will be cooled by 48 coolant channels of 8 mm diameter. Flow is in poloidal direction so that the power input to each channel is equal. Each cooling cell consisting of two flow channels connected in series is 28 mm wide.

The copper finger is attached to the stainless steel support plate by stainless steel pins of 4.5 mm diameter located at a pitch of 12 mm.

To reduce the flow velocity and flow rate required to cool the outer divertor, a swirl tube is used to increase the critical heat flux. The swirl tape thickness is 1.5 mm and twist ratio is 2. The swirl tape will be used only in the high heat flux area of the divertor (~ 50% length).

### **4.3.3. RESULTS**

A flow velocity of 10 m/s gives sufficient safety margin on CHF for the divertor. If two adjacent channels are connected in series, the maximum outlet temperature is 95°C and exit pressure is 1.00 MPa, resulting in a minimum subcooling of 87°C. The CHF on the coolant channel wall under these conditions is 44 MW/m<sup>2</sup>. The flow per module is 9 ℓ/s.

A three dimensional FE analysis of a divertor finger was performed for these flow conditions.

The reference design shows a distance of 4 mm between the coolant channel and the PFC. Thermal and stress results for this geometry are shown in column 1 of Table 4.3.3. The copper temperature, thermal stress in the copper and shear stress on the pins is too high.

An alternate design with 3 mm distance between coolant channel and PFC was also analyzed. The remaining five stress-reducing measures listed in the introduction will be analyzed in FY02.

**TABLE 4.3.3**  
**Analysis Results for Two Geometries**

	Reference Design (4 mm)*	Modified Design (3 mm)*
Maximum Cu Temperature, °C	502	455
Maximum W Temperature, °C	1470	1412
Maximum Stress in Cu, Mpa	643	580
Maximum Force on Assembly Pins, N	15633.	14601
Maximum Shear Stress in the 4.5 mm pins @ 12 mm pitch, Mpa	982	917
Maximum Allowable Shear Stress, Mpa	220	220
Maximum Coolant Channel Wall Heat Flux (MW/m <sup>2</sup> )	26.3	27.4
Safety Margin on CHF	1.67	1.6

\*Distance between coolant channel and PFC.

**Section 5**

---

**ADVANCED LIQUID PLASMA-FACING SURFACES (ALPS)**

## 5. ADVANCED LIQUID PLASMA-FACING SURFACES (ALPS)

During this fiscal year we coordinated tokamak experiments in CDX-U and DIII-D. Analysis of the disruptive Li-DiMES exposure results from DIII-D showed that the behavior of the injected liquid Li is caused by MHD effects and is consistent with the results from pellet injection of Li into the DIII-D core. We also supported the ALPS project modeling group tasks with the use of MCI code to model the transport of impurities from the chamber surface to the plasma.

### TOKAMAK EXPERIMENTS

We coordinated the liquid metal exposure experiments in CDX-U and DIII-D. Initial experiments were performed in CDX-U with the UCSD liquid lithium limiter. Results showed that with a fresh solid lithium limiter, hydrogen recycling of the lithium wall was much reduced but not eliminated. Argon glow discharge cleaning (GDC) was found to be most effective in cleaning the liquid lithium limiter surface, which is reflected in the best vacuum pump out rate. Lithium-I emission was clearly seen when the lithium was interacting with the plasma. The effect of lithium gettering of oxygen was clearly shown. Droplets of lithium were occasionally observed with the liquid lithium limiter, but no disruptions occurred. Comparison with the DIII-D disruptive DiMES results, reported below, indicates this could be due to the relative low electron temperature of the CDX-U plasma, which allows a relatively long lithium ablation mean free path, reducing the deposition and ionization of the lithium in the plasma core.

A toroidally continuous lithium tray at the lower divertor was fabricated. Experiments with this lithium tray will provide crucial information on the possible MHD interaction of the lithium with the plasma, when the liquid lithium is toroidally continuous and electrical and thermal contacts between the melted lithium and the stainless steel tray are much higher than in the Li-DiMES experiment described in the following.

We successfully exposed a lithium DiMES sample in DIII-D to varying divertor heat loads by gradually moving the outboard strike point towards the plasma. Measurements indicate that the physical sputtering of lithium is sufficiently low for it to be considered as an acceptable plasma-facing material in the tokamak. However, we have seen strong effects from the displacement of liquid surface due to  $\mathbf{J} \times \mathbf{B}$  MHD effects. On all the MHD interactions, including earlier experiments, essentially all solid lithium coatings were heated to liquid state by the plasma, removed and distributed to the surrounding surface and into the plasma core.

For the experiment performed in March of this year, movement of the liquid lithium and the emission of neutral and ionized lithium radiation in the scrape off layer, in the divertor region and in the core were clearly recorded from very different plasma discharges. The injection of lithium into the plasma core in a low power L-mode discharge and the resulting locked mode disruption were most unexpected. The source of the driving current density ( $J$ ) in the lithium is the tokamak parallel current which could be enhanced by its interception with the non-uniformity (ripples) of the lithium surface. This low power L-mode experiment also indicated an enhanced impact of lithium radiation in the core when the plasma temperature was  $> 1$  keV. There was a detrimental effect on the energy balance of the plasma core, providing a plausible explanation of why radiation collapse was not observed in CDX-U and T11-M experiments when lithium droplets were passing through the core.

The low power L-mode plasma discharge was analyzed carefully. One of the key diagnostics used for this analysis was the DIII-D tile current array located at the same major radius as the DiMES sample and as the SPRED system, which monitors the time evolution of the lithium radiation in the core plasma. The observed reduction and recovery of the tile current indicates modification and re-establishment of the parallel current at about the time when the lithium melts. This confirms that the parallel current is the source of current density ( $J$ ), which caused the movement of the liquid lithium on the DiMES sample leading to the enhanced  $J \times B$  effect that injected the lithium into the plasma core.

The enhancement of  $J$  in the melted lithium is possibly due to interception of the parallel current by mm-scale non-uniformity of the lithium surface. This non-uniformity could be caused by the initial lithium movement over the lid of the lithium cup.

It is of interest to note that the injected lithium blob behaves much like an injected lithium pellet. The timing and quantity of radiation in the core and the resulting locked mode, energy deposition and ionization in the plasma core are quite similar to what has been observed and analyzed with lithium pellet injection. More description and analysis of this experiment is given in Section 7, Plasma Interactive Materials.

## **Li-DiMES MODELING**

We have been focusing on an MCI Li transport analysis during the disruptive phase of a Li-DiMES experiment. Preliminary estimates of the Li neutral mean free path show that very little Li should reach the core prior to the observed enhanced Li release phase. A simple model of Li-transport does not appear to explain the sudden increase in core Li

content. Again, comparison with similar effects resulting from lithium pellet injection may provide the explanation. More analysis is presented in Section 7, Plasma Interactive Materials.

We are also using the MCI code to model the transport of lithium before the disruptive discharge.

## **ATOMIC DATA COORDINATION**

Progress was made in getting both ADAS and ADPAK lithium data loaded into a DiMES-relevant background plasma solution for MCI modeling runs. A complete set of ADAS electron impact ionization data for  $\text{LiI} \rightarrow \text{LiII}$ ,  $\text{LiII} \rightarrow \text{LiIII}$  and  $\text{LiIII} \rightarrow \text{LiIV}$  at five densities was supplied to J. Brooks at ANL for benchmarking with DIII-D experiments.

## **CONFERENCES/MEETINGS**

T. Evans chaired a session on plasma material interactions at the Lithium Mini-Conference held during the Quebec APS meeting.

## **PUBLICATIONS/REPORTS**

Two ALPS project reports, “Exposure of Solid and Liquid Lithium in the DIII-D Tokamak” and “The Analysis of a DIII-D Disruption Sequence Induced by a Small Lithium Sample Subjected to a Low Power L-mode Plasma,” were completed and sent to ANL. The reports are accessible from the ALPS web site.

Section 6

---

**ADVANCED POWER EXTRACTION STUDY (APEX)**

## 6. ADVANCED POWER EXTRACTION STUDY (APEX)

During this fiscal year we coordinated APEX Task IV: the High Temperature Refractory Solid Wall, First Wall (FW) and Blanket evaluation. We completed evaluation of the EVOLVE FW and blanket design, including transpiration and boiling blanket options. We assisted in carrying out a successful peer review. We completed the assessment of the SiC<sub>f</sub>/SiC (SiC fiber in an SiC matrix) composite LiPb cooled blanket. Ferritic steel and Flibe were proposed as the structural and self-cooled tritium breeder materials to be assessed under the APEX program for next year.

### EVOLVE DESIGN

We completed evaluation of a transpiration-cooled, i.e., cooling by vaporized lithium through capillaries on the wall, FW and blanket design by including the poloidal and toroidal flow FW configuration and blanket options. We found that due to the shorter length of the vapor flow path the vapor velocity at the corresponding outlet of the blanket is much lower for the poloidal design, which is shown in Fig. 6.1. The overall pressure drop and the resulting capillary diameter of the toroidal flow FW concept are very sensitive to an increase in the B-poloidal to B-toroidal magnetic field ratio ( $B_p/B_T$ ). The poloidal flow channel concept allows a larger margin on the lithium superheat uncertainty. It also allows more freedom on the selection of blanket tray geometry. To address the uncertainty in the lithium superheat data, we proposed a heat transfer experiment that could be used to study the one-sided heating of the transpiration-cooled tube. We also investigated an insulated double wall feeding tube option, which is acceptable in terms of energy loss and pressure drop. Furthermore, we proposed a hybrid system with vertical vapor channels formed by a capillary sheet structure, which may help to reduce the problem of high void fraction in the boiling blanket option.

Critical issues of the EVOLVE design are the superheating of lithium for the transpiration-cooled FW/blanket design, boiling stability in the magnetic field for the boiling blanket approach, and the robustness of the capillary sheet FW for both blanket concepts.

The final report of the EVOLVE design is nearly complete.

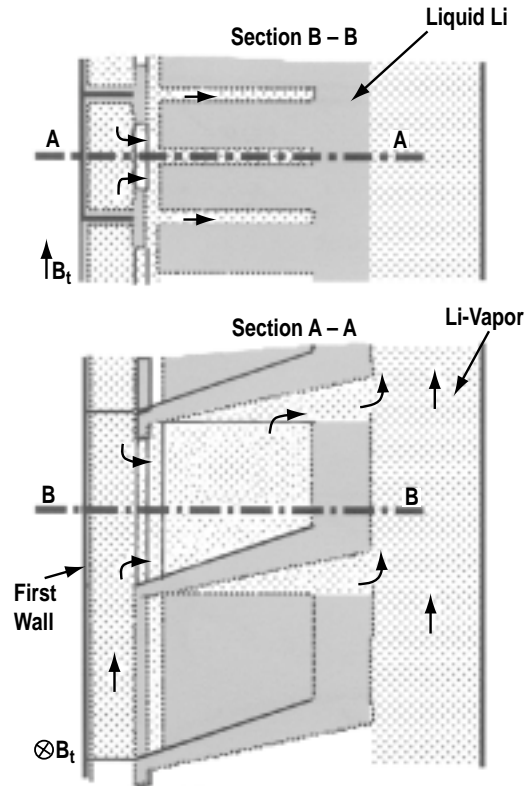


Fig. 6.1. Schematics of the poloidal flow transpiration cooled EVOLVE FW/blanket design.

## SiC<sub>f</sub>/SiC-LiPb DESIGN ASSESSMENT

The tasks for the multi-institutional evaluation of the SiC<sub>f</sub>/SiC-LiPb FW/blanket design were formulated and reviewed by the team. S. Malang of FZK visited GA to work on the evaluation of the SiC<sub>f</sub>/SiC composite structural material and LiPb breeder and coolant FW/blanket design.

We performed a simple thermal hydraulics analysis of the SiC<sub>f</sub>C/SiC-LiPb FW/blanket module and found that the thermal conductivity and the maximum allowable operating temperature of the SiC<sub>f</sub>/SiC material will be the key limiting factors to the module performance. Accordingly, we have been focusing the assessment on the projected range of the thermal conductivity and on other feasibility issues, such as projected material lifetime, performance of leak tight composite and compatibility between SiC<sub>f</sub>/SiC composite and LiPb. The assessment of SiC<sub>f</sub>/SiC composite lifetime was difficult due to the lack of material properties and of an available analysis code.

Others have performed local and global modeling of C<sub>f</sub>/C composite without the interface coating. We proposed the use of the finite elements ANSYS code to model detailed material properties change of fiber, coating and matrix materials. This might be

an appropriate method to identify radiation damage on the composite material and to show ways of improving the materials. Using this approach, we completed the first computation with a one-fiber element before extending the method to a more complicated local structure. The one-fiber model has also been used by PNL coupled to a more traditional local/global model method. Our one-fiber model, combined with ANSYS code results, matched well with the experimental measurement of the Si<sub>3</sub>N<sub>4</sub> composite push-out test.

Evaluation of the extended thermal performance of the ARIES-AT FW and blanket is nearing completion. The University of Wisconsin (UW) duplicated the results that were obtained at UCSD. Smolentsev (UCLA) generated a more detailed LiPb coolant channel velocity profile with the inclusion of MHD effects. Murphy (UW) is using this velocity profile for the poloidal and helical flow calculations.

## **CHAMBER TECHNOLOGY PEER REVIEW**

We assisted in carrying out a successful chamber technology peer review that was held at UCLA. Task IV results were presented.

## **PLANNING FOR FY02**

S. Malang visited GA and helped review future work under Task IV, beyond the SiC<sub>f</sub>/SiC LiPb cooled concept. It was agreed that the basic approach should be the use of advanced ferritic steel as the structural material and FliBe as the breeder and coolant. This approach was reviewed and approved by the APEX team as the basis for FY02 Task IV work

## **CONFERENCES/MEETINGS**

1. C. Wong visited Chinese fusion research facilities. Three new toroidal machines are being built: the spherical torus machine ( $R_o=0.3$  m) at Tsinghua University, the superconducting HT-7U machine ( $R_o=1.6$  m) at ASIPP, and the normal conducting HL-2A machine ( $R_o=1.64$  m) at SWIP. A list of proposed U.S./PRC exchange items were gathered and transmitted to OFES.
2. C. Wong attended the KTM (Kazakhstan Tokamak Materials testing) device meeting at Astana, Kazakhstan. This device is about the size of NSTX and has an aspect ratio of 2. It will have a unique, completely movable lower divertor that can be rotated 360° and can be raised from the lower position to the mid-plane of the device for divertor components exchange. This device is to be funded by the

Kazakhstan government and is scheduled to operate by the end of 2003. It will cost \$15M to \$20M, not including diagnostics.

3. C. Wong presented a paper at the IAEA meeting in Sorrento, Italy, on “Toroidal Reactor Design as a Function of Aspect Ratio”.
4. C. Wong presented the paper on “The Evaluation of the Tungsten Alloy Vaporizing Lithium FW and Blanket Concept” at the 14th ANS Topical Meeting on the Technology of Fusion Energy in Park City, Utah.

**Section 7**

---

**PLASMA INTERACTIVE MATERIALS (DiMES)**

## 7. PLASMA INTERACTIVE MATERIALS (DiMES)

During this fiscal year we continued to use the Divertor Materials Evaluation System (DiMES) to develop an integrated experimental database on plasma-material interaction in tokamaks. We performed erosion and transport studies on solid and liquid surface materials. We found that the MHD interaction of the induced current in the liquid metal with the magnetic field can inject the conducting liquid into the plasma core and create a disruption. We continued to work on the erosion database of C and W as plasma facing material. We measured scrape off layer properties and identified a credible scheme of disruption mitigation by massive injection of inert gas.

### 7.1. Li EXPERIMENT

A DiMES Li-sample was exposed to well-controlled L-mode plasmas in DIII-D. Steady Li radiation was observed and the plasma performance was not degraded until the strike point was moved close to the sample. The estimated heat flux was still relatively low at  $< 0.5 \text{ MW/m}^2$ . A large amount of Li was transported and detected in the core. Subsequently, a disruption was induced and the remaining Li on the sample surface was removed due to the  $\mathbf{J} \times \mathbf{B}$  force. These results raise serious concerns about the viability of using liquid lithium surfaces in a tokamak reactor.

Experimental data were provided to UCLA for MHD modeling of the lithium injection into the plasma core. Initial results indicated surface movement of the liquid metal and a change in current density in the fluid. The model will be refined to simulate the effect of the vertical injection of lithium into the plasma core from the lower divertor. Further experiments can then be proposed to find ways to avoid the detrimental effects.

#### 7.1.1. EXPERIMENTAL BACKGROUND

A DIII-D DiMES sample was designed to accommodate a 2.54 cm diameter lithium sample contained within a 1.3 mm deep graphite holder (approximately 350 mg of lithium). The lithium sample consisted of multiple layers of a thin, high purity, lithium foil pressed into the graphite holder. A sequence of four plasma discharges were run in which the outer strike point of a low power, lower single-null, L-mode discharge was swept slowly across the lithium sample. The goal was to heat the lithium sample slowly then study sputtering and transport properties as a function of the sample temperature. In particular, detailed information about the lithium plasma-surface interaction and about

transport properties near and just above the solid-to-liquid phase transition boundary was desired.

Only the first swept strike point case showed any signs of melting or increased Li radiation. It is possible that during the first swept shot the individual layers of lithium foil may have briefly melted. After completing the four swept outer strike point discharges, the plasma was positioned with the outer strike point fixed approximately 3 cm from the center of the lithium sample. All of the shots in this experimental sequence were run with a toroidal magnetic field of 2.05 T, a plasma current of 1.2 MA, an ohmic heating power of 1.1 MW, a neutral beam heating power of 2.6 MW and an elongation of 1.7.

### 7.1.2. EXPERIMENTAL DATA

The complete set of DIII-D lower divertor diagnostics were used to record the details of the plasma density and temperature and the evolution of Li radiation. Of particular interest are the row 13 tile current array (TCA) monitors located close to the DiMES sample. These monitors are comprised of three individual detectors centered at a major radius  $R=1.48$  m (the same radius as the center of the DiMES probe) but separated toroidally to measure the toroidal distribution of the SOL current flowing parallel to the magnetic field. The row 13 TCA monitors are located at toroidal angles  $\phi = 45^\circ, 135^\circ, 310^\circ$ . They spatially integrate the current flowing in the SOL and private flux region over a 13 cm wide radial extent. Parallel currents in the SOL can be generated by electron temperature difference at the ends of the flux tubes connecting the inner and outer divertor target plates in lower single-null plasmas. Typically,  $T_e$  at the outer strike point is higher than that of the inner strike point causing a thermoelectric current ( $j_{th}$ ) to flow out of the low field side target plates, over the top of the plasma, and into the high field side target plates. The circuit is completed through the vacuum vessel toroidally and poloidally.

During the plasma current plateau of the first shot, each of the row 13 TCA monitors registered a relatively steady net negative current (positive  $j_{th}$ ) of 10–15 A/tile until about 3416 ms into the shot.

Figure 7.1 shows the signals from the three row 13 TCA monitors during the final 85 ms of the shot (upper frame) and the evolution of the plasma current during this time (lower frame).

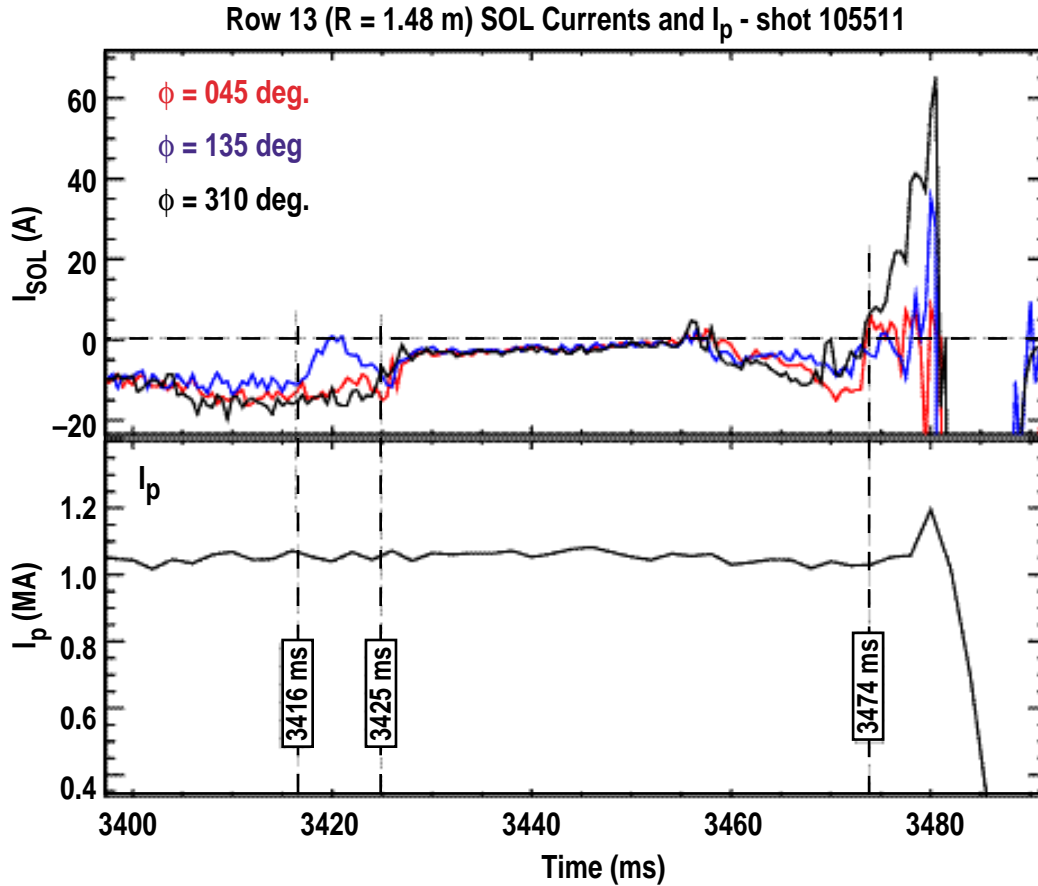


Fig. 7.1. Upper frame: Tile current array monitor signals in the row 13 tiles during the termination phase of shot 105511. Lower frame: Plasma current during the final 85 ms of the shot.

Note that during the onset of the current termination sequence,  $3474 \text{ ms} < t < 3480 \text{ ms}$ , the SOL current develops a relatively large negative non-axisymmetric halo-like current component which may be due in part to an increase in a negative  $j_{th}$  component (i.e., into the tile) during a vertical displacement event and the subsequent thermal quench. Following the thermal quench, plasma current in the core ( $I_p$ ) begins to drop at approximately the L/R decay rate of a 100 eV plasma and a large positive halo current forms (not displayed in the upper frame of Fig. 7.1 in order to emphasize the behavior of the SOL current earlier in the shot). These  $I_p$ -quench-induced halo currents are not driven by the thermoelectric effect. They are driven by the collapse of the poloidal magnetic flux and can reach peak values ranging from 25%–45% of the plasma current when integrated toroidally and poloidally.

Following the drop to zero at 3420 ms, the current flow out of  $\phi = 135^\circ$  TCA monitor begins to build up again. At the same time the signals on the other row 13 TCA monitors start to decay. By 3425 ms the SOL currents have reestablished their original axisymmetric distribution and are all decaying toward zero. By this point in the discharge

we believe the lithium cloud has spread out enough to cover most of the divertor and SOL. The lithium radiation has likely equilibrated  $T_e$  spatially and is driving it to lower values uniformly around the SOL, which globally reduces the driving potential for  $j_{th}$ . After  $t = 3427$  ms,  $j_{th}$  is essentially zero everywhere in the SOL, and thus can no longer produce any significant  $j_{th} \times B$  forces on the plasma facing components or on the lithium sample.

As  $T_e$  drops in the divertor ( $t > 3427$  ms) it appears that a detached-like state is reached across the entire divertor region with very little heat flux reaching the target plates or the lithium sample. The signals in the row 13 TCA monitors (upper frame of Fig. 7.1) begin to rise again slowly at about 3455 ms following a 25 ms decay from about 5 A/tile to zero. This increase results from the growth of a locked mode on the  $q = 2$  surface, which first appears on the pr12 and pr13 locked mode detector signals at 3452 ms (see the upper frame of Fig. 7.2). Various types of locked and resistive wall modes are commonly observed on the TCA monitor signals but the signals shown between 3455 and 3474 ms in the upper frame of Fig. 7.2 are unusual. Locked modes usually produce non-axisymmetric thermal electric current with amplitudes of 50–100 A/tile rather than the 10–20 A/tile seen on this shot. This difference may be attributed to a build up in the lithium density throughout the SOL and into the outer core region of the plasma. The lithium radiation should moderate the power flow from the core into the divertor and reduce the thermoelectric potential needed to drive  $j_{th}$ .

The upper frame of Fig. 7.2 clearly shows the onset of a growing locked mode at 3452 ms compared to the earlier, relatively featureless, behavior of the pr12 and pr13 signals prior to that point. In the lower frame of Fig. 7.2, the increase in the deuterium recycling at approximately the same radial location as the DiMES probe and the row 13 TCA monitors confirms the growth of the locked mode. This signal suggests that the locked mode destroys the core confinement inside the  $q = 2$  surface and some of the heat and particles get dumped from the core into the divertor. While the lithium in the core moderates the magnitude of the heat flux reaching the divertor targets, it does not completely eliminate it during the locked mode.

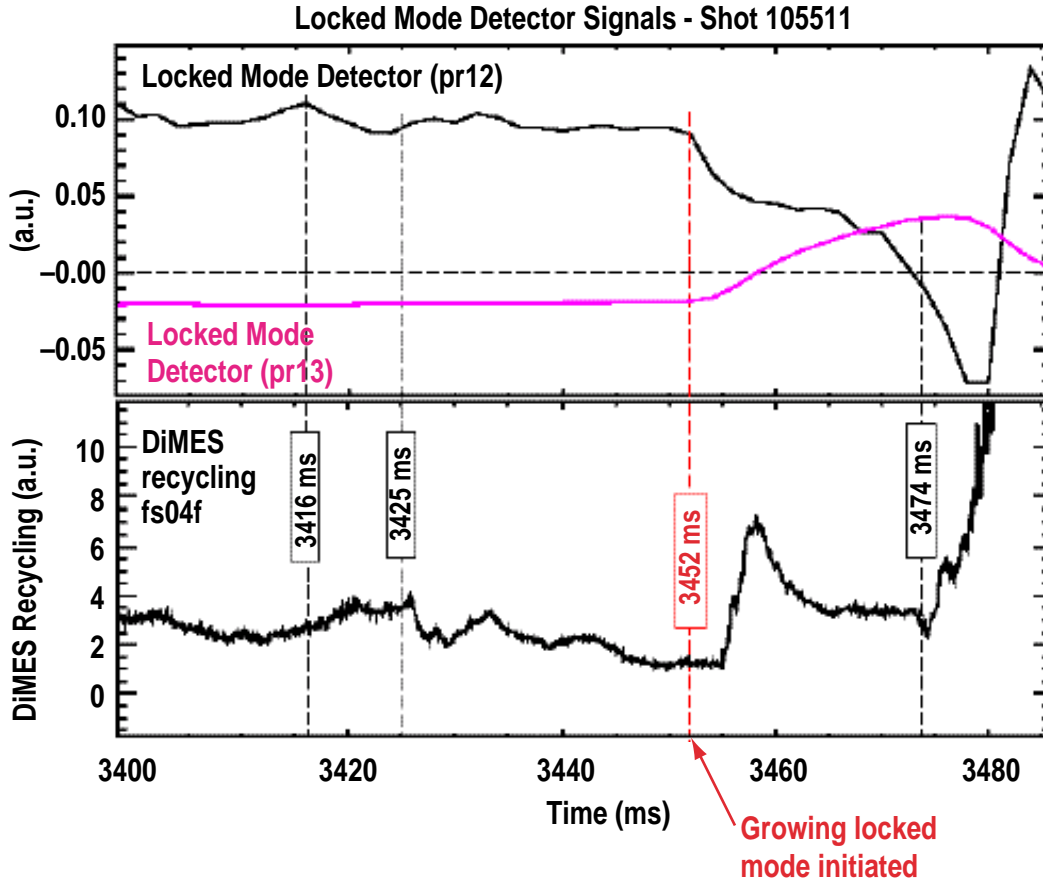


Fig. 7.2. Upper frame: locked mode detector signals pr12 and pr13 show the onset of a growing locked mode at 3452 ms. Lower frame:  $D_{\alpha}$  recycling light from filterscope chord looking near the DiMES probe shows an increase in recycling as the locked mode grows after 3455 ms.

As the locked mode depletes the stored kinetic energy inside the  $q=2$  surface, the plasma beta drops and the DIII-D vertical control system is unable to prevent the plasma from moving toward the inner wall of the vessel. This triggers a rapidly growing vertical displacement event at approximately 3478 ms (about the time that  $I_p$  starts to increase as the internal inductance of the plasma changes due to a current profile redistribution), which drives the plasma downward until the X-point contacts the lower divertor target plates (somewhere in the vicinity of the DiMES probe). Once the X-point touches a lower divertor surface, a rapid thermal quench dumps the remainder of the plasma's stored kinetic energy into the SOL and lower divertor. This initiates the  $I_p$  quench in which all the energy in the poloidal magnetic field is converted to kinetic energy and deposited on the plasma facing surfaces. The current quench also inductively drives large non-axisymmetric halo currents in the SOL, which are measured with the TCA arrays. These currents can be seen in the signals of the row 13 TCA monitors (upper frame of Fig. 7.1) starting at 3480 ms where the signals switch polarity from positive (current

flowing into the tiles) to negative (current flowing out of the tiles). The full amplitude of the signals has been cut-off in the figure to emphasize the earlier features starting at about 3416 ms. The halo current induced during the  $I_p$  quench in this shot was about 600 A/tile.

An inspection of the data from the DIII-D CO<sub>2</sub> laser interferometer chords shows that the core electron density,  $n_e$ , started to increase slowly ( $dn_e/dt = 6.9 \times 10^{20} \text{ m}^{-3} \text{ s}^{-1}$ ) from  $2.5 \times 10^{19} \text{ m}^{-3}$  at 3428 ms until  $t = 3444$  ms and then increased at a more rapid rate to  $6.1 \times 10^{19} \text{ m}^{-3}$  at 3458 ms. A solid lithium fragment (or liquid droplet) with a radius of approximately 1.6–2.6 mm (10–40 mg of lithium) would be required in order to cause this increase in  $n_e$ . The size of the lithium droplet cannot be accurately determined due to the uncertainty in the charge state distribution of the lithium in the core.

Separate analysis of data from these experiments suggests that the disruption sequence was most likely initiated by the injection of a single large blob of liquid lithium, moving at approximately 30 m/s, which penetrated about 35–40 cm into the core plasma before burning out.

### 7.1.3. SUMMARY

The sequence of events recorded in DIII-D can be divided into three distinct phases. The first involves the initial ejection of the lithium blob, which probably accounts for loss of about 5%–10% of the initial mass of the sample. The second involves the heat flux and current from the locked mode which probably accounts for the removal of another 20%–30% of the initial mass. The third phase involves the disruptive thermal quench and halo currents which probably accounts for the removal of the remaining 60%–75%. Each of these phases involve complex physics phenomena that are not completely understood. Additional experimental measurements are needed, and development of more advanced theoretical tools will be required, to fully assess the feasibility of liquid metals as plasma facing materials in high heat flux regions, particularly when SOL currents are also present.

We are working with the UCLA modeling group to understand the MHD effects leading up to the injection of lithium into the core. Initial results indicated the surface movement of the liquid metal and the change in current density in the fluid. The model will be refined to simulate the effect of the vertical injection of lithium into the plasma core from the lower divertor. Further experiments can then be proposed to find ways to avoid the detrimental effects.

## 7.2. SCRAPE-OFF LAYER MEASUREMENT

DIII-D SOL properties were measured during single-null L-mode discharges with symmetric (in magnetic flux space) inner and outer gaps. A broadening of the density profile was observed as the central density increased. Detailed comparisons of the L-mode SOL and Far-SOL profiles of C-Mod and DIII-D showed striking similarities in the trends and absolute values of plasma transport. It was found that as the line-averaged density was increased, the effective diffusivity and cross-field transport was greatly enhanced in the Far-SOL. This will significantly impact the erosion of chamber wall materials. Further investigations are needed.

## 7.3. SOLID TARGET EXPERIMENTS

A hazardous work authorization (HWA) covering the use of a Be-coating and the exposure of high-Z materials was submitted and approved by DIII-D management. A DiMES multi-materials sample was then exposed, as a piggyback experiment, to more than 10 low power limited discharges. Diagnosis of the DiMES location showed weak plasma flux to this region compared to neutral flux, inferred from pressure gauges. The sample was analyzed at Sandia National Laboratories and results showed minimum material erosion and redeposition. We plan to repeat this experiment with the addition of Sn coating and with exposure to a higher number of plasma discharges.

## 7.4. DISRUPTION MITIGATION

High-pressure gas injection of neon was used to simultaneously mitigate disruption thermal loading and control runaway electron amplification, both major concerns for next-step tokamaks. The neon was injected into a plasma that was above the no-wall stability limit and approaching an ideal kink limit disruption. Preliminary analysis confirmed several aspects of our modeling: good penetration, predominantly low charge-state for the neon, and a cold resistive plasma with a fast current quench and little or no runaway electron current amplification. The gas injection mitigation left the wall well conditioned, as evidenced by the absence of injected impurities and low radiated power in the breakdown of the subsequent discharge. We propose to repeat this experiment with the injection of argon gas in FY02.

## 7.5. W-ROD EXPERIMENT

After initial rejection by the DIII-D planning committee, a technical note was prepared to explain need for a W-rod experiment and to explain the precautions taken to minimize the risk of DIII-D vessel contamination. Approval was given to propose the W-rod experiment for FY02.

## 7.6. PLANNING FOR FY02

Ten proposals for the 2002 DIII-D experimental campaign, including four for dedicated experiments, were presented at the DIII-D brainstorming meeting. These proposals cover experiments with high-Z surface materials, including W-rod, multi-layer coating and W-arc; lithium transport at the FW and divertor; leading-edge and FW materials erosion assessment; effect of injected impurities on divertor surface erosion; and diagnostics development.

## 7.7. CONFERENCES/MEETINGS

- The DiMES program was represented at the IAEA meeting in Sorrento, Italy. The paper "The Effect of Detachment on Carbon Divertor Erosion/Redeposition in the DIII-D Tokamak," was presented by D.G. Whyte.
- D. Whyte presented "Studies of SOL Transport and Recycling on DIII-D," at the SOL Transport Workshop held in Fairbanks, Alaska.
- D. Whyte attended the IAEA-TCM on Divertor Concepts in Aix-en-Provence, France and gave a presentation on "Observations on the Location, Mechanism and Consequences of Impurity Generation in the DIII-D Tokamak."

## 7.8. PUBLICATIONS/REPORTS

- D.G. Whyte et al, "The Effect of Detachment On Carbon Divertor Erosion/Redeposition in the DIII-D Tokamak," accepted for publication in Nucl. Fusion.
- D.G. Whyte, D.A. Humphreys and P.L Taylor, "Measurement of Plasma Electron Temperature and Effective Charge During Tokamak Disruptions," Physics of Plasmas, Vol. 7, p. 4052.

**Section 8**

---

**VANADIUM COMPONENT DEMO**

## 8. VANADIUM COMPONENT DEMO

A paper entitled “Effects of Tokamak Exposure of Vanadium Alloys,” by H. Tsai (A~L), Y. Yam (ANL), W. Johnson (GA), A. Bozek (GA), P. Trester (GA), J. King (ORNL), and D. Smith (ANL), was submitted and accepted for presentation at the 10th International Fusion Materials conference held in Boden-Boden, Germany. The paper was presented by Dr. Tsai.

Dr. W. Robert Johnson (GA) was invited by the National Institute of Fusion Science (NIFS) in Toki, Japan to attend the Second U.S./Japan Workshop on the Technology of Large-Scale Production of Low-Activation Vanadium Alloys. Dr. Johnson presented information on the status of vanadium alloy ingot and product form production, and vanadium alloy joining technologies. Workshop presentations in similar areas were made by NIFS personnel and representatives of Japanese industry engaged in vanadium alloy production.

### CONFERENCES/MEETINGS

1. Second U.S./Japan Workshop on the Technology of Large-Scale Production of Low-Activation Vanadium Alloys, Tokai, Japan, June, 2001.

### PUBLICATIONS/REPORTS

1. H. Tsai, Y. Yam, W. Johnson, A. Bozek, P. Trester, J. Kin, and D. Smith, “Effects of Tokamak Exposure of Vanadium Alloys,” 10th International Fusion Materials Conference, Boden-Boden, Germany, October 14-19, 2001.

**Section 9**

---

**RF TECHNOLOGY**

## 9. RF TECHNOLOGY

### COMBLINE ANTENNA

During FY01, continued discussions on comblin antenna design were held with staff of Japan's National Institute of Fusion Science (NIFS) and with Prof. Takase of the University of Tokyo. NIFS has a collaboration with Prof. Takase to assist in the design and fabrication of a comblin antenna for the LHD device. NIFS is considering a comblin antenna to be located in the high magnetic field region of the stellerator to achieve good coupling with the electrons for fast wave current drive.

Dr. Charles Moeller met with Prof. Y Takase and Drs. T. Watari, R. Kumazawa and T. Seki (NIFS-LHD) in Japan November 19–22, 2000. The purpose of the visit was to determine how to feed the balanced LHD comblin antenna with a single coax or stripline at the input and output, while exciting a symmetric current distribution in the radiating elements. Prof. Takase has made a 4-strap comblin for testing the concept. The coupling approach selected during the visit was to use a symmetric closed loop to inductively couple both halves of the end elements, regardless of the support. The feed is a direct tap to an experimentally-determined point on one half of an element. It was determined experimentally that this coupling approach could adequately separate the anti-symmetric mode pass band from the symmetric mode pass band, and that a region of low reflectivity could be achieved in the symmetric mode pass band. This was determined experimentally by incorporating sliding end cap extensions to the end elements since they needed to be electrically longer to make up for the effect of the coupling loops. Prof. Takase was pleased with the progress made during the visit and expressed interest in further collaboration.

### ADVANCED ECH LAUNCHER DEVELOPMENT

Improved launcher mirror concepts with enhanced heat removal capability are being developed. The design developed during FY01 uses a copper-plated carbon fiber composite (CFC) mirror with a high thermal conductivity flexible carbon fiber bundle heat pipe emanating from the backside of the mirror. Thermal analyses show that a DIII–D size mirror can reflect 800 kW for about 2 min before the hottest spot exceeds 200°C, with a starting temperature and heat sink temperature of 35°C. The carbon fiber bundle diameter in this design is 6 cm, and the fiber length is 20 cm. With a larger bundle of fibers to the heat sink, true CW can be achieved.

A proof-of-principle CFC disk with an integral bundle of fibers emanating from the back was received from the vendor. This mirror was designed to fit a standard DIII-D miter bend frame for testing. The fiber bundle diameter for this experiment was only 1.3 cm in order to keep costs within budget. An attempt was made to coat the front face of the CFC disk with a thin layer of copper, but the coating did not adhere properly. To make a better surface for the copper to adhere to, the assembly was returned to the vendor, where a dense CVD carbon layer was deposited on the surface. However, because of concerns about the CVD layer cracking during thermal cycling, a second prototype mirror was fabricated. In this new mirror, a graded CVD carbon/CFC layer was produced at the mirror surface. A separate flexible carbon fiber bundle with CFC segments at the ends was also produced. This will be used with the CFC mirror or with a small metal mirror to demonstrate its ability to remove heat from the mirror to a heat sink. A photograph of both the graded CVD/CFC mirror and the flexible carbon fiber bundle are shown in Fig. 9.1.



*Fig. 9.1. Photograph of the prototype graded CVD/CFC mirror and flexible carbon fiber bundle under development for use in advanced long pulse ECH launcher mirrors.*

In a related area, GA has continued to develop the remotely-steerable launcher concept. JAERI, which has considerable interest in the concept as an ECH launcher for ITER, purchased from GA a prototype launcher suitable for high power tests at 170 GHz using evacuated launcher waveguide. The apparatus included a water-cooled rotating

mirror housed in a five-way cross vacuum chamber and a 4.6 m long, square cross section evacuated waveguide. As part of the U.S./Japan RF Technology Exchange, GA performed low power tests on the apparatus at GA and participated in low and high power tests in Japan in November 2000 and January 2001. The apparatus set up at JAERI for high power tests is shown in Fig. 9.2.

JAERI made radiation pattern measurements using both long and short pulses of approximately 400 kW incident power for several steering angles. In the initial measurements, it was found that the radiated power fell off more rapidly with increasing steering angle than predicted by calculations. There also appeared to be relatively high power reflected back into the chamber housing the rotating mirror. These effects were attributed to periodic non-uniformities in the corrugation depth in the square cross section waveguide and to distortions in the waveguide straightness which occurred during shipping. The initial tests in Japan were performed with electric field polarized in the plane of steering, a configuration for which steering behavior is much more sensitive to the corrugation geometry than for H-field in the plane of steering. Subsequently, low power tests were performed at GA on a proof-of-principle apparatus designed for operation at 110 GHz. With E-field in the plane of steering, the predicted radiation pattern was observed on this apparatus which has very uniform corrugation geometry.

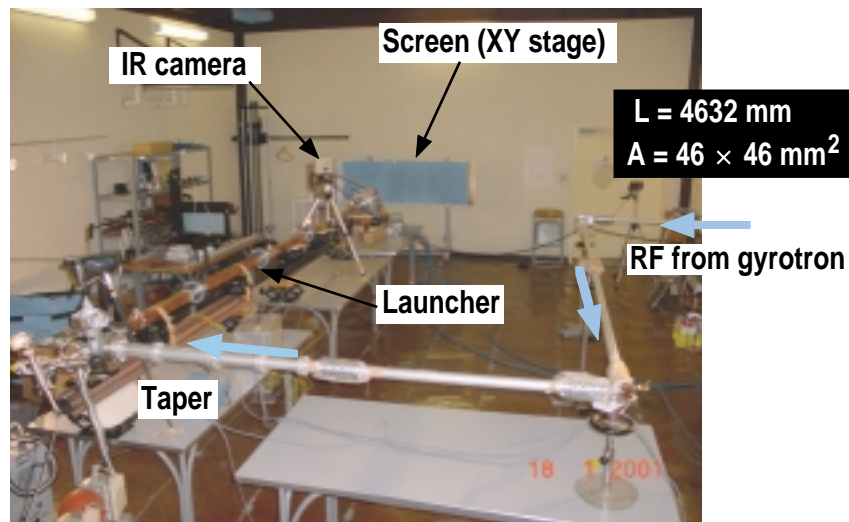


Fig. 9.2. Experimental set-up at JAERI for high power testing of the 170 GHz remotely-steerable launcher apparatus.

Subsequent low and high power tests were performed at JAERI after the waveguide was straightened. The new radiation pattern measurements showed improved behavior compared to measurements made in January 2001, in that the radiated power did not fall

off nearly as rapidly with increasing steering angle as in the earlier measurements. Measurements were made both with the electric field polarized in the plane of steering and perpendicular to the plane of steering. With the electric field perpendicular to the plane of steering, the falloff was only 2% and 5% at steering angles of 5° and 10°, respectively.

Based on the promising results with the first prototype launcher, JAERI decided to purchase a new prototype remotely steerable launcher apparatus with improved waveguide straightness and dimensional uniformity and with an improved mirror rotation and translation mechanism. Tests on this improved system should confirm the key high power performance characteristics of the remotely steerable launcher concept.

## **WINDOW VALIDATION**

Over the last year there have been a number of failures of CVD diamond windows on DIII-D and other gyrotrons. A better understanding of the CVD window fabrication and operational procedures is required in order to have reliable operation of 1 MW 10 s gyrotrons. Failed CVD diamond windows have been sent to Germany for measurements of loss tangents, and it has been found that loss tangents of brazed windows range from 2 to 8 times that of the virgin CVD diamond disks. Significant variables appear to be brazing temperature and brazing environment which can cause graphitization of the diamond surface, with a consequent increase in apparent loss tangent. GA has been developing a diagnostic for measuring the loss tangent of CVD diamond disks, both as bare disks and as mounted in a brazed fixture. The concept is to insert the diamond in a resonant cavity to determine the change in cavity Q. The cavity being built consists of a corrugated waveguide with parallel copper mirrors mounted at each end, with small coupling holes in each mirror to launch and detect 110 GHz HE<sub>11</sub> mode microwaves. The cavity is cut in the middle to insert the diamond disk or disk assembly. The axial position of the mirrors can be adjusted so that the diamond can be located in a region of maximum electric field. The expected periodicity of the resonances when the mirror spacing was changed by multiples of one-half wavelength was not initially observed, although suitably high Q resonances were found. Improving the flatness of the mirrors by hand lapping them made the periodicity more apparent, however. The next step is to have the mirrors machined very flat using a diamond bit to eliminate any remaining curvature; subsequent polishing will not be required.

While continuing to refine the closed cavity approach, an alternate approach using confocal mirrors in an open cavity configuration was investigated. The remainder of the translation, microwave, and data acquisition apparatus can remain the same for either

type of cavity. The main potential advantage of the open cavity over the closed waveguide cavity is that introducing the diamond disk into a gap in the waveguide changes the radiation from the gap. The diamond actually reduces the loss, but a correction must be made for this change, even though it is small. In the open cavity, conversely, as long as the diamond disk is very flat, the radiation losses are not changed. The open cavity is also sensitive to mirror imperfections, however, although they only show up as a reduced Q, with a corresponding lower sensitivity.

A method under consideration for enhancing the sensitivity of the loss tangent measurements, applicable to either cavity, is to place low-loss dielectric disks one-quarter wavelength from either the mirrors (this should reduce their loss by  $\epsilon$ , the dielectric constant of the disk), or on each side of the diamond disk (this should increase the absorption by the diamond by a factor  $\epsilon$ ).

## **INTERNATIONAL COLLABORATION**

The 19th U.S./Japan RF Technology Exchange was held at PPPL from October 30 to November 1, 2000. There were 26 attendees, including 11 from Japan. A total of 26 technical presentations were given to describe the status of U.S. and Japan rf programs and to propose continued and new U.S./Japan collaborations. GA staff made presentations on DIII-D gyrotron performance, carbon fiber composite ECH launcher mirror development, remote steering launcher development, and combine antenna design. A total of 17 collaborations were proposed for Japanese FY01, with the specific details to be worked out by the U.S. and Japan counterparts. The Proceedings of the 19th U.S./Japan RF Technology Exchange were printed and distributed to the attendees.

Douglas Remsen attended the 16th Topical Meeting on RF Power in Plasmas, held in May 2001 at Oxnard, California. Members of the international rf community were present. At this meeting, Mr. Remsen met with several directors of fusion facilities in Europe to discuss the possibility of having bilateral rf technology exchanges as we have had for the last 19 years with Japan and the last 5 years with Korea. It appears as though the proposal was met with agreement, and we await their responses in order to start working out the details.

The tentative dates for the next U.S./Japan RF Technology Exchange are from February 28 through March 2, 2002. The host will be the National Institute for Fusion Science (NIFS). The exact location has not yet been determined, but it is expected to be in the Nagoya area. It is hoped that the Japan/Europe RF Technology Exchange Meeting can be held simultaneously in order to have greater technical exchange among the parties. On the last day the meeting would break up into bilateral exchange meetings for

discussions on progress on bilateral collaborations and proposals for possible new collaborations.

## **CONFERENCES/MEETINGS**

1. The 19th U.S./Japan RF Technology Exchange Workshop, Princeton, New Jersey, October 30–November 1, 2000.
2. 16th Topical Meeting on RF Power in Plasmas, Oxnard, California, May 7–9, 2001.

**Section 10**

---

**SPIN-OFF BROCHURE**

## 10. SPIN-OFF BROCHURE

Over the last fifty years the pursuit of fusion energy has led to the development of materials, processes, codes and understanding of basic plasma physics that have found many applications in scientific and engineering fields outside of the fusion arena. GA has written a brochure illustrating ways that fusion science and technology have influenced and contributed to these other fields. The brochure is twenty pages long and targets the interested but non-technical person, with an effort to provide a basic understanding of the fusion process and of the contribution fusion research has had on other technologies and scientific areas. In addition to the normal “spin-off” topics usually applied to such literature, the concept of highly trained experts as a spin-off commodity has been included. The migration to other research fields by fusion experts, with their broad understanding of the very complex phenomena occurring in the study of heated plasmas, may be the largest impact fusion research has had on other scientific fields.

The title of the brochure is “The Suprising Benefits of Creating a Star.” After the introduction the brochure gives a brief description of the three known methods of achieving conditions for sustained fusion to occur. The next part of the brochure covers the areas of physical science that have seen contributions from the fusion program. High density material science, advanced diagnostics and nonlinear chaotic system behavior are identified as areas with much synergism. The remainder of the brochure covers technology spin-offs, such as space travel, semiconductor circuit fabrication, material processing, medical and health applications, and pollution reduction and remediation.

Twenty thousand copies of the brochure have been printed and are being distributed to interested parties. Hundreds of brochures were given out at this year’s Educational Outreach Forum held at the 43rd Annual American Physical Society Conference held in Long Beach, California.

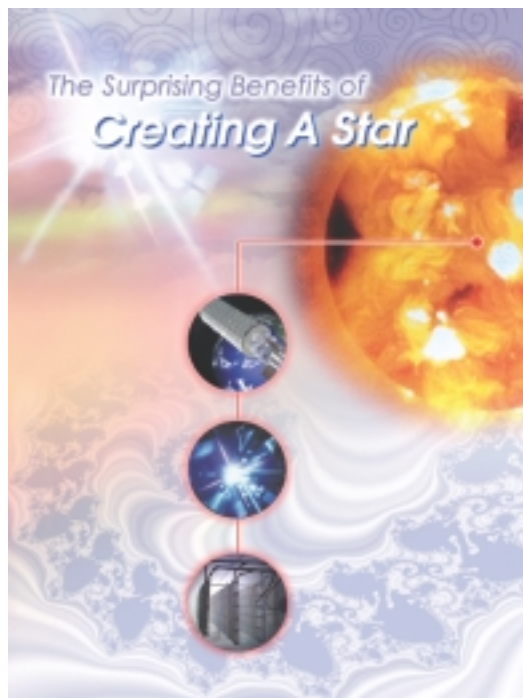


*Fig. 10-1. Cover of spin-off brochure.*